Mon. Not. R. astr. Soc. (1989) **241**, 707–720

Infrared spectroscopy of dust in the Taurus dark clouds: solid carbon monoxide

D. C. B. Whittet,[1,2,3] A. J. Adamson,[1] W. W. Duley,[2] T. R. Geballe[4] and A. D. McFadzean[5]

[1] *School of Physics and Astronomy, Lancashire Polytechnic, Preston PR1 2TQ*

[2] *Physics Department, York University, 4700 Keele Street, Downsview, Ontario, Canada M3J 1P3*

[3] *Canadian Institute for Theoretical Astrophysics, University of Toronto, 60 George Street, Toronto, Ontario, Canada M5S 1A1*

[4] *Joint Astronomy Centre, 665 Komohana Street, Hilo, Hawaii 96720, USA*

[5] *School of Physics and Space Research, University of Birmingham, PO Box 363, Birmingham B15 2TT*

Accepted 1989 May 19. Received 1989 May 17

Summary. Spectra centred on the spectral feature of solid CO at 4.67 μm wavelength are presented for eight stars in or behind the quiescent dark cloud complex in Taurus. The solid CO profile is dominated by a sharp component (FWHM ~ 8 cm^{-1}) centred at 4.673 μm (2140 cm^{-1}). As in previous observations of the feature, asymmetry in the profile is consistent with the presence of a weaker, somewhat broader, overlapping component centred at ~ 4.682 μm (2136 cm^{-1}). New and previously published data for Taurus stars are combined to study the correlation of the peak optical depth in the CO feature with visual extinction and with the depth of the water-ice feature at 3.0 μm. A threshold extinction of $A_V = 5.3 \pm 0.6$ mag is required for solid CO to be of detectable strength, compared with 3.3 ± 0.1 for water-ice. CO embedded in an H_2O matrix may explain the broad component of the feature, but cannot account for the dominant sharp feature. The best correspondence to the latter is obtained with CO embedded in non-polar molecules such as CO_2 or CH_4. Comparison of our data for solid CO with gas-phase column densities deduced from millimetre-wave observations of CO emission in the same lines-of-sight suggests that ~ 30 per cent of the available CO is depleted on to grains.

1 Introduction

The possibility that solid CO might be a vital constituent of grain mantles was first suggested by Duley (1974), a prediction confirmed observationally some 10 years later. The 4.67-μm C≡O 'stretch' feature of solid CO has now been observed in a number of lines-of-sight, including

young stellar objects embedded in molecular clouds (Lacy *et al.* 1984; Geballe 1986) and background field stars observed through the extensive dark-cloud system in Taurus (Whittet, Longmore & McFadzean 1985, hereafter Paper I). Recent observations of the Serpens cloud (Eiroa & Hodapp 1989) and the ρ Oph complex (Whittet *et al.*, in preparation) confirm the ubiquity of the feature in dense interstellar environments. Because of its status as the most abundant gas-phase molecule to exhibit a rotational spectrum at normal ambient temperatures in molecular clouds, the abundance and depletion of interstellar CO are topics of considerable significance and current debate (see, for example, van Dishoeck & Black 1987). Millimetre-wave observations of CO are widely used to map the distribution of molecular material in the interstellar medium, and the column densities of CO (and hence H_2) will be underestimated if a significant fraction of CO resides in the solid state on grains. In addition to its importance as a tracer of molecular material, CO is vital to the production of many polyatomic molecules by gas-phase reaction schemes, and the depletion of CO could therefore be a limiting factor for chemical models for the gas as well as the grain mantles. Further motivation for studying the 4.67-μm feature of solid CO is provided by laboratory results, which indicate that details of the profile (precise position, width and shape) are sensitive to the chemical nature of the mantle as a whole and to the extent of any thermal processing (Maki 1961; Sandford *et al.* 1988; Schmidt, Greenberg & Grim 1989). The feature thus has great potential as a diagnostic of both chemical and physical conditions.

The Taurus dark clouds provide an ideal laboratory in which to investigate the nature of grain mantles in a quiescent environment (Whittet 1987; Adamson *et al.* 1988). Whittet *et al.* (1983) were first to demonstrate that the 3.0-μm water-ice feature is easily detectable in field stars observed through these clouds, given a visual extinction $A_V \geq 3$–4 mag. A detailed study of the ice and 9.7-μm silicate features was carried out by Whittet *et al.* (1988, hereafter Paper II). In the current paper, we present 4.6–4.75-μm spectra for eight of the sources included in Paper II, thus extending our preliminary study of solid CO in this region presented in Paper I. New and previously published data are combined to investigate the correlation of the CO feature strength with visual extinction and water-ice absorption, and to estimate the degree of depletion. A comparison of the position and width of the observed feature with laboratory data is used to place constraints on the composition of the mantles.

2 The spectra

The observations were made on the nights of 1986 December 1 and 2, with the cooled grating spectrometer CGS2 on the United Kingdom Infrared Telecope (UKIRT) at Mauna Kea Observatory in Hawaii. A grating ruled with 300 lines mm^{-1} was used to give spectra of resolution $\Delta\lambda \simeq 0.0063$ μm centred at 4.67 μm in the first order. The wavelength scale was calibrated relative to an argon lamp and is accurate to ± 0.003 μm. An aperture of diameter 5 arcsec was used throughout. Cancellation of telluric features and subsequent flux calibration was achieved by ratioing the coadded spectral scans with corresponding scans of standard stars observed at similar air mass, and then multiplying the spectrum by a blackbody function corresponding to the temperature of the standard star. It is usual to select bright stars of intermediate spectral type as standards, as their spectra are relatively featureless in the wavelength range considered here. However, several of our programme stars are late in spectral type (K and M), and are therefore expected to have intrinsic gas-phase CO features in their spectra, comprising unresolved lines in the P and R branches of the fundamental vibration–rotation band; as we are concerned here only with the interstellar features, we included late-type stars in our standards list in order to attempt cancellation of the stellar component. In most cases, we found that the shape, depth and width of the solid CO feature is not, in fact, strongly dependent on the spectral type of the standard used.

The programme stars, standard stars and their spectral types are listed in Table 1. The spectral types of the programme stars are from Elias (1978) and Paper II, those of the standard stars from the *Bright Star (BS) Catalogue*. The final spectra, shown in Figs 1 and 2, have been Hanning-smoothed, resulting in a ~25 per cent degradation in resolution, i.e. to $\Delta\lambda \simeq 0.008\ \mu$m (3.5 cm^{-1}). It is clear from inspection of Figs 1 and 2 that the solid CO feature at 4.67 μm is present in several of the spectra, and is prominent in Elias 15 and Tamura 8. There are no other strong features. The Pfβ line of hydrogen at 4.654 μm is present in emission in Elias 1, consistent with its classification as an Ae star; this feature is not evident in any other spectra presented here. A previous spectrum of Elias 1 obtained with the same instrumentation (Paper I) agrees with that in Fig. 1(a) to within observational error; the present spectrum is of higher signal-to-noise ratio and is used in all subsequent analyses.

As first noted by Lacy *et al.* (1984), the profile shape of the observed 4.67-μm feature is consistent with the presence of two overlapping features, a 'broad' component centred at ~2136 cm^{-1} (4.682 μm) and a 'narrow' component centred at ~2140 cm^{-1} (4.673 μm). In our spectra, the profiles are dominated by the narrow component, although the broad feature (which appears as a long-wavelength 'wing') is also discernible, given adequate optical depth and signal-to-noise ratio. It is most prominent in Tamura [(Fig. 2c).

3 Optical depths and linewidths

3.1 RESULTS

In this section, we include results for spectra presented in Paper I in addition to those described in Section 2 above. Three parameters of the 4.67-μm feature were deduced for each star: (i) the peak optical depth, $\tau_{4.67}$, measured relative to a linear continuum drawn through points adjacent to the feature (4.60–4.64 and 4.70–4.75 μm), (ii) the full-width half maximum, $\Delta\nu_{1/2}$, measured from a linear intensity plot, and (iii) the wavelength at maximum optical depth, λ_0. No attempt was made to separate the broad and narrow components of the feature referred to above. Results for $\tau_{4.67}$ and $\Delta\nu_{1/2}$ are listed in Table 2, along with derived column densities (see Section 4.1). The measurements of λ_0 show no significant variation from star to star about a mean value of $4.673 \pm 0.002\ \mu$m.

3.2 ANALYSIS AND DISCUSSION

Fig. 3 shows a plot of $\tau_{4.67}$ (Table 2) against A_V (Paper II and references therein). Embedded members of the cloud population (Elias 1, 7 and 18; HL Tau) are distinguished from

Table 1. Stars observed.

Programme star	Spectral type	Standard star*
Elias 1	A6e	2, 3
Elias 3	K2 III	1
Elias 6	M8 III	4
Elias 14	M5 III	4
Elias 15	M2 III	3, 4
Elias 23	T Tau	2, 3
Tamura 8	K5 III	1, 3
HD29647	B7 IVp	2, 3

*Standard stars:

1. BS489 (K3 III),
2. BS1017 (F5 Ib),
3. BS1373 (K0 III),
4. BS8775 (M3 II–III).

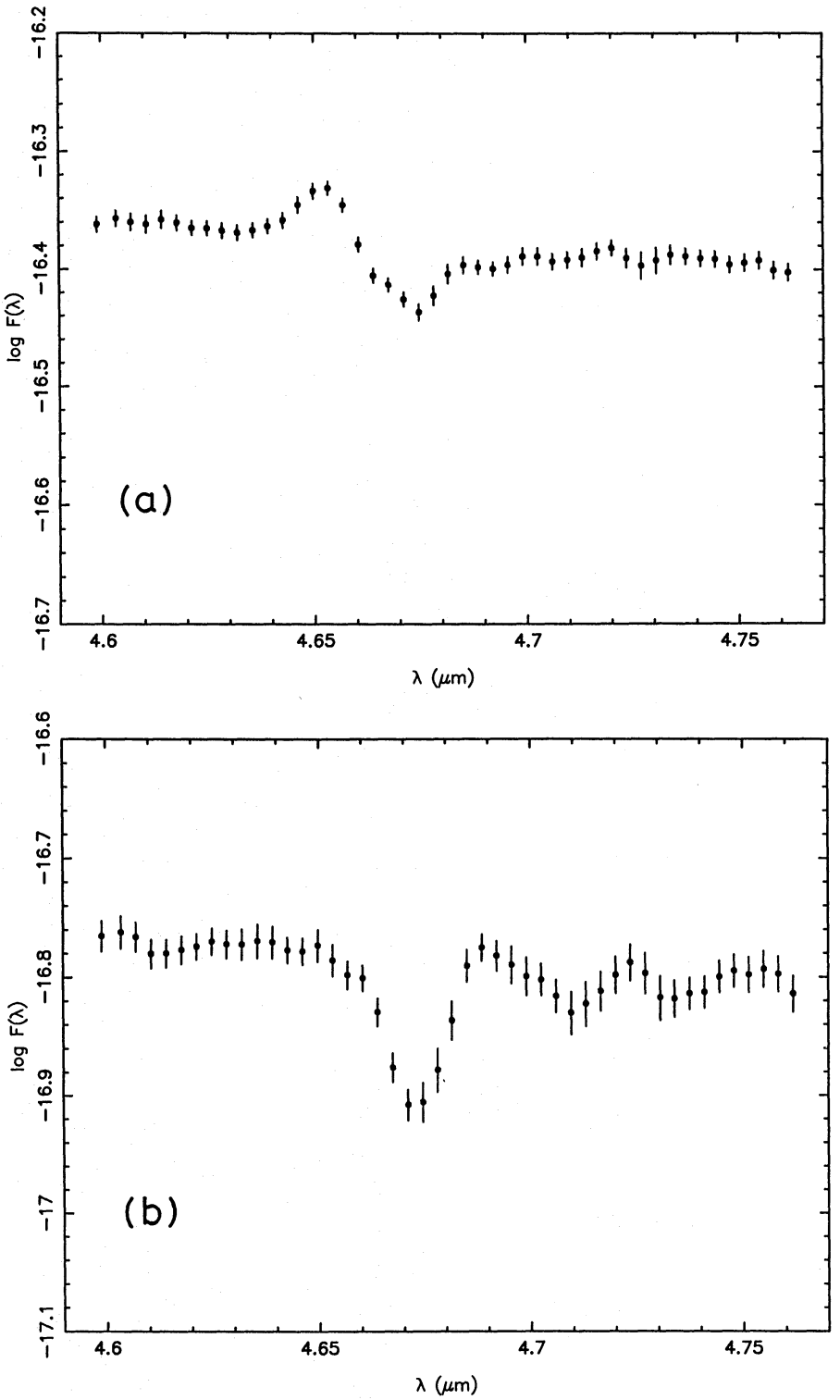

Figure 1. Spectra from 4.60–4.76 μm for (a) Elias 1, (b) Elias 3, (c) Elias 6 and (d) Elias 14. Flux $F(\lambda)$ is in units $\mathrm{W\,cm^{-2}\,\mu m^{-1}}$.

background field stars by a different plotting symbol. A good linear correlation is evident, with only Elias 18 deviating significantly from the general trend. As discussed elsewhere (Paper II; Adamson *et al.* 1988), the extinction towards this object may have been overestimated. Omitting Elias 18, a linear least-squares fit to the points for stars with solid CO detections

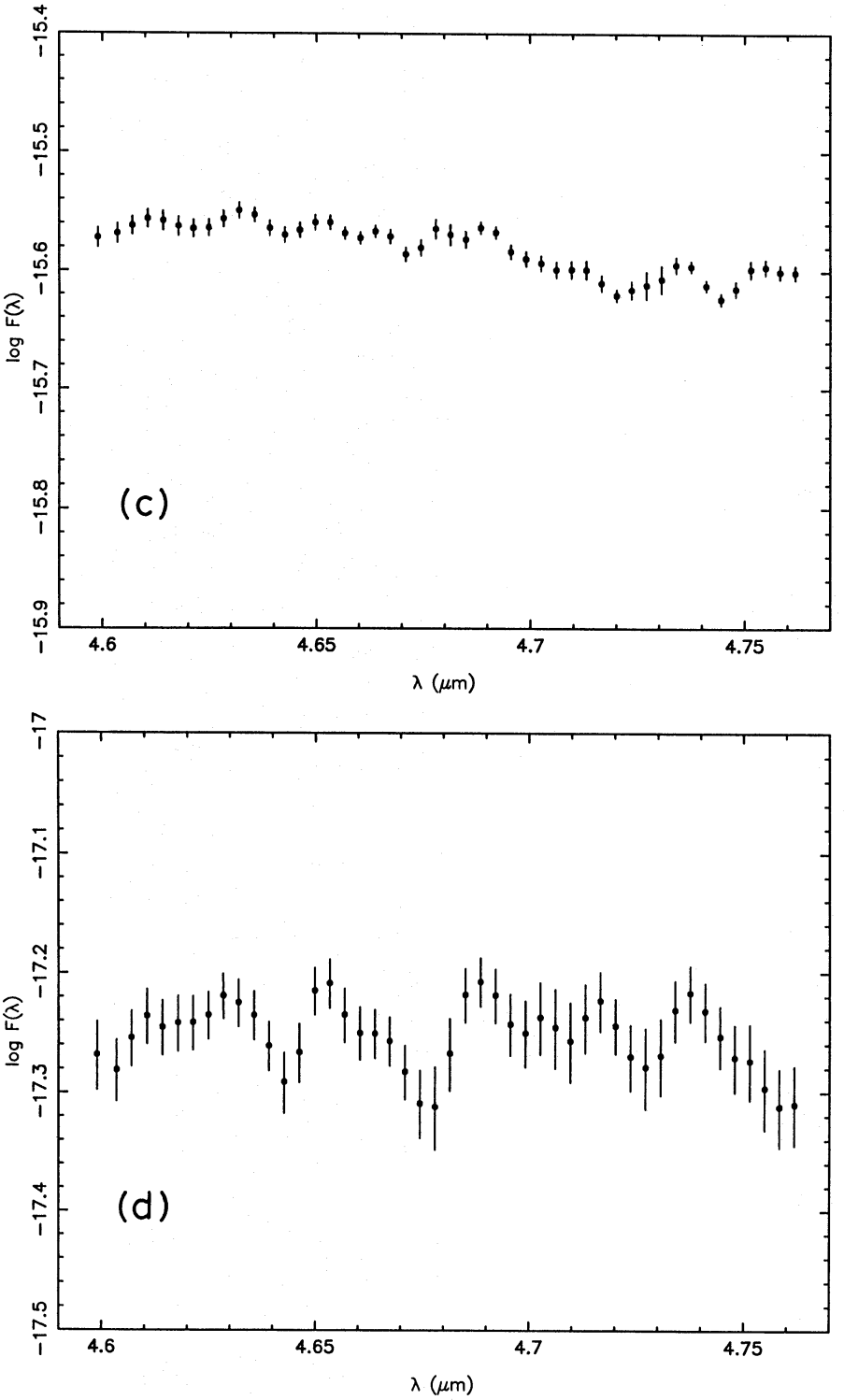

Figure 1 – *continued*

gives the result

$$\tau_{4.67} = 0.064(A_V - 5.9). \quad (1)$$

If Elias 1 and 7 are also excluded (leaving only field stars), the resultant fit is

$$\tau_{4.67} = 0.058(A_V - 4.7). \quad (2)$$

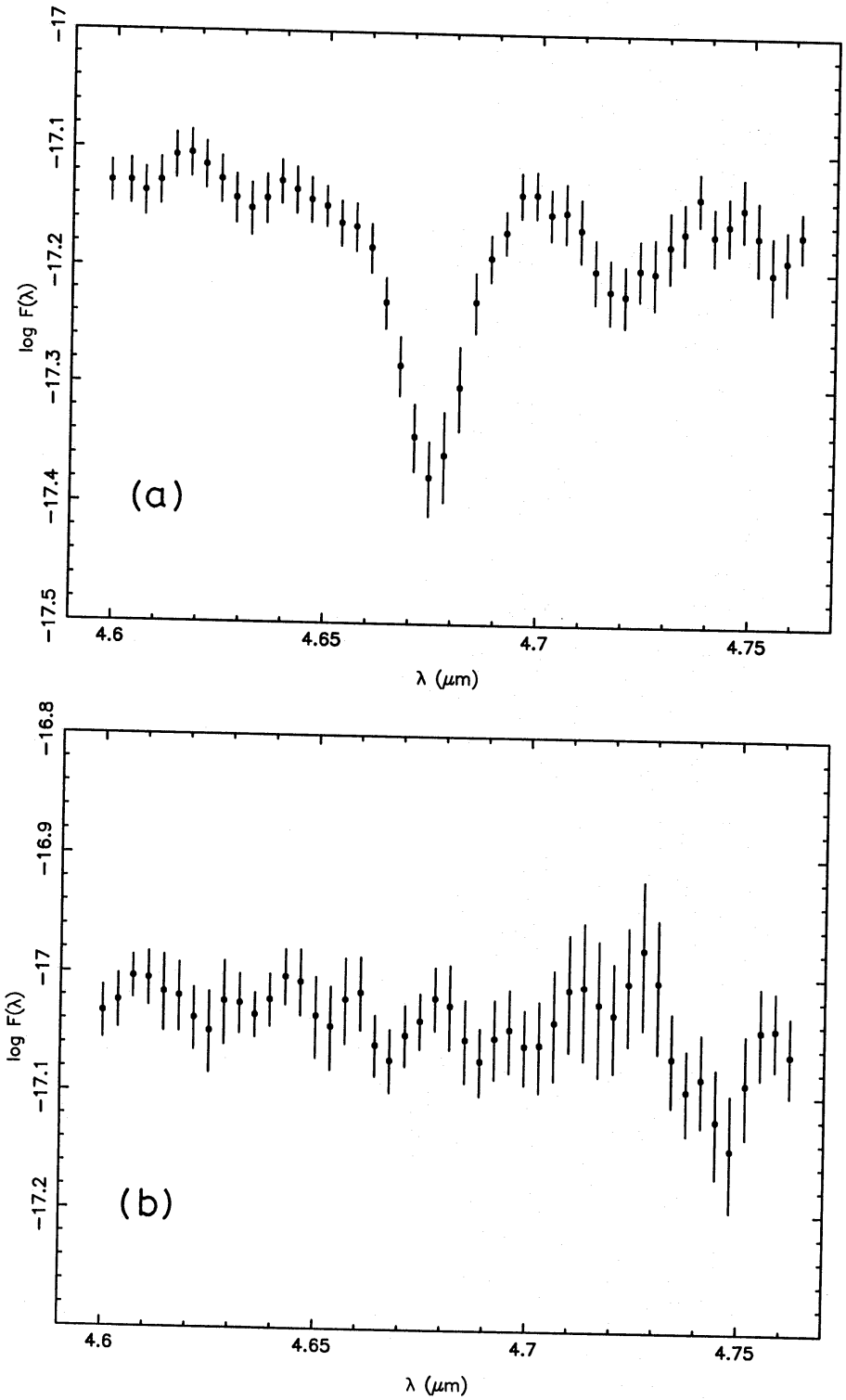

Figure 2. Spectra from 4.60–4.76 μm for (a) Elias 15, (b) Elias 23, (c) Tamura 8 and (d) HD29647. Flux $F(\lambda)$ is in units W cm^{-2} μm^{-1}.

Thus, a threshold extinction of $A_V \sim 5$ mag appears to be required to provide an environment sufficiently shielded from the external radiation field for CO to survive on grain mantles; we adopt $A_V = 5.3 \pm 0.6$ as the most probable value of this threshold. In comparison, the threshold for detection of water-ice in Taurus is $A_V = 3.3 \pm 0.1$ (Paper II).

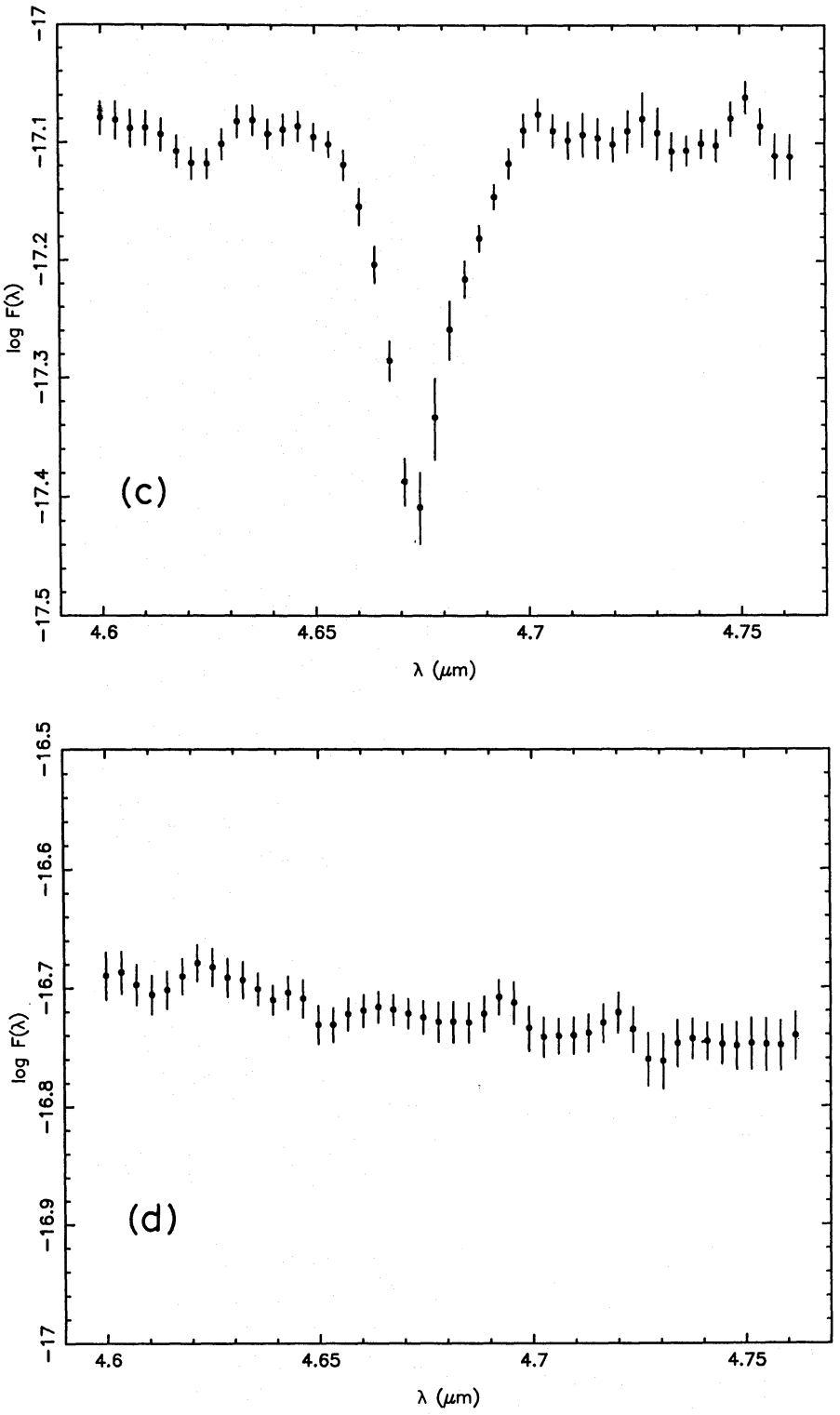

Figure 2 – *continued*

Fig. 4 shows a plot of $\tau_{4.67}$ against the peak optical depth, $\tau_{3.0}$, measured for the 3.0-μm water-ice feature (Paper II). Disregarding the upper limits, the overall degree of correlation is remarkably high ($r \simeq 0.98$). A linear least-squares fit to the field stars gives the relation

$$\tau_{4.67} = 0.69(\tau_{3.0} - 0.25). \quad (3)$$

Table 2. Observational results.

Star*	$\tau_{4.67}$	$\Delta\nu_{\frac{1}{2}}$ (cm^{-1})	$N_{dust}(CO)$ ($\times 10^{17} cm^{-2}$)
Elias 1	0.14 ± 0.04	7.8 ± 1.5	1.1
Elias 3	0.29 ± 0.07	7.4 ± 1.2	2.1
Elias 6	< 0.04	—	< 0.3
Elias 7	0.13 ± 0.06	~ 10	~ 1.3
Elias 13	0.22 ± 0.06	7.5 ± 1.5	1.7
Elias 14	< 0.16	—	< 1.3
Elias 15	0.53 ± 0.07	8.6 ± 1.2	4.6
Elias 16	0.96 ± 0.06	7.0 ± 0.6	6.7
Elias 18	0.35 ± 0.06	11.3 ± 1.2	4.0
Elias 23	< 0.10	—	< 0.8
Tamura 8	0.74 ± 0.06	8.6 ± 1.0	5.8
HD29647	< 0.06	—	< 0.5
HL Tau	< 0.05	—	< 0.4

*Data for Elias 7, 13, 16, 18 and HL Tau are based on spectra published in Paper I.

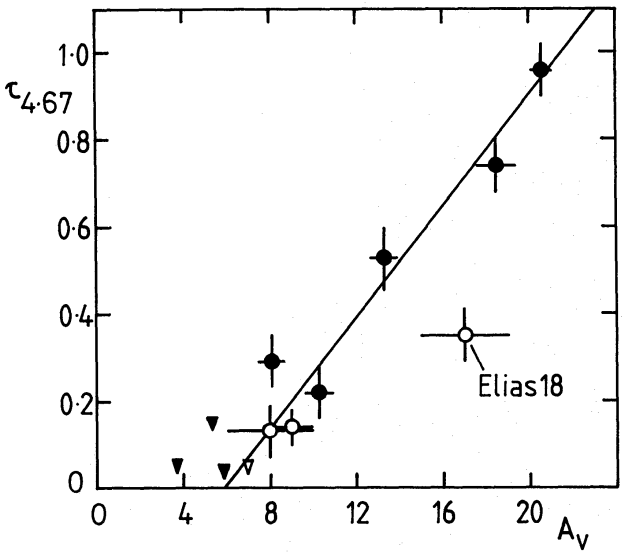

Figure 3. Plot of peak optical depth in the 4.67-μm solid CO feature against visual extinction. Open symbols represent dust-embedded stars, filled symbols field stars. The straight line is a least-squares fit (see equation 1 in the text).

The small positive intercept on the $\tau_{3.0}$ axis indicates the existence of a cloud layer in which water frosts condense whilst the more volatile CO remains in the gas.

Comparing Fig. 3 with Fig. 4, Elias 18 occupies a normal position in the latter, which supports the view that its anomalous position in the former is simply due to an overestimate of A_v. There is no significant difference in the distribution of field and member stars in Fig. 4, with the notable exception of HL Tau, which has strong water-ice absorption but no detection of solid CO. It is well known that much of the extinction towards this star arises in an edge-on circumstellar disc in which grain temperatures are typically 100–300 K (Paper II and references therein). Thus, the absence of solid CO is not surprising. It appears that the $\tau_{4.67}$ versus $\tau_{3.0}$ diagram for a given cloud may provide a useful discriminator between objects with cool protoplanetary shells or discs and objects with normal molecular cloud extinction.

As previously noted, the width and peak wavelength of the CO feature are sensitive to the composition and thermal history of the mantle. Figs 5 and 6 show plots of the width parameter

$\Delta\nu_{1/2}$ against $\tau_{4.67}$ and λ_0, respectively. There is no clear evidence for any systematic trend in width as a function of depth into the cloud (Fig. 5): only Elias 18 deviates by more than 1σ from the mean value of $\Delta\nu_{1/2} = 7.7 \pm 0.5\,\mathrm{cm}^{-1}$ for the field stars (dashed line). Fig. 6 compares the mean observational result for field stars (cross) with laboratory data for various ice mixtures measured at 10 K (Sandford *et al.* 1988). Pure CO ice produces a feature near 4.676 μm which is significantly narrower than observed ($\Delta\nu_{1/2} \simeq 2.5\,\mathrm{cm}^{-1}$). All mixtures in which the dominant constituent is water-ice produce a feature with $\lambda_0 \simeq 4.681\,\mu$m and $\Delta\nu_{1/2} \simeq 10\,\mathrm{cm}^{-1}$ (box at top right in Fig. 6): the difference in λ_0 compared with the observed

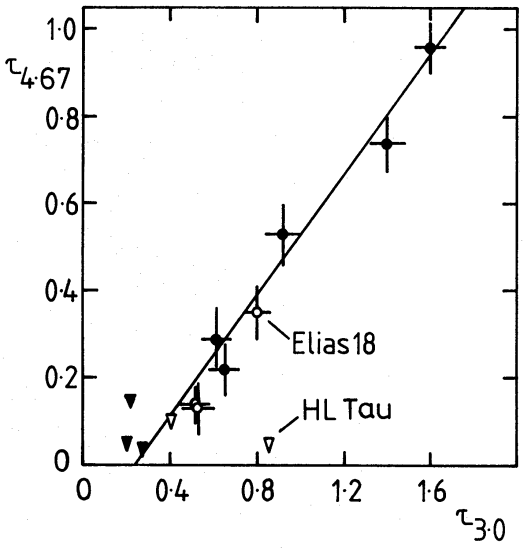

Figure 4. Plot of peak optical depth in the 4.67-μm solid CO feature against that in the 3.0-μm ice feature. Open symbols represent dust-embedded stars, filled symbols represent field stars. The straight line is a least-squares fit (see equation 3 in the text).

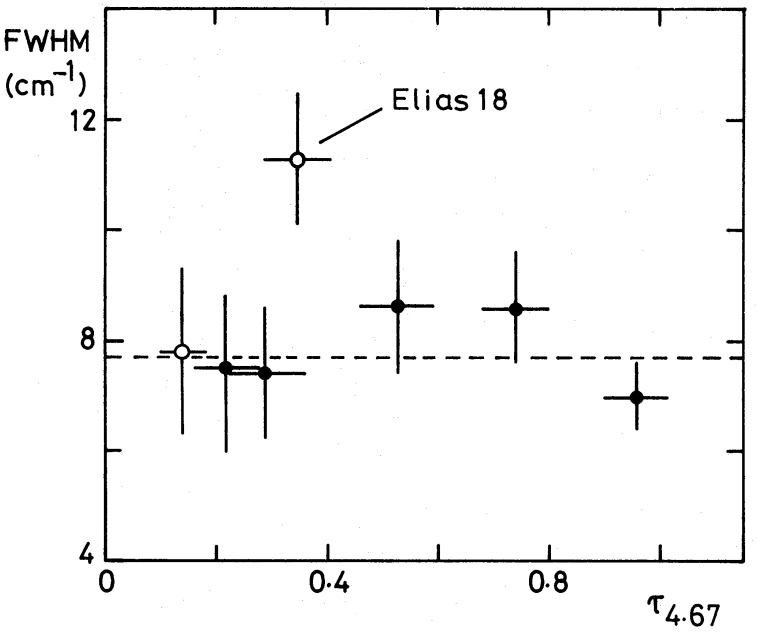

Figure 5. Plot of FWHM against peak optical depth for the solid CO feature. The dashed line represents the mean value for field stars (filled circles); embedded objects are represented by open circles.

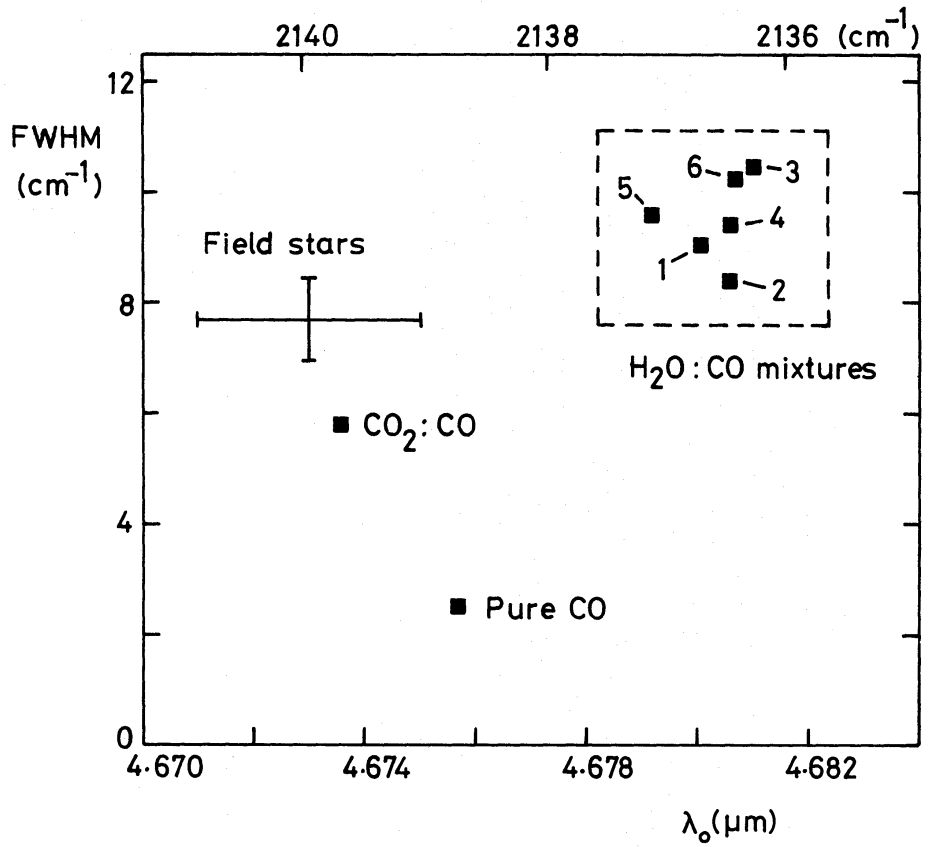

Figure 6. Plot of FWHM against the wavelength of peak absorption in the solid CO feature, comparing the mean observed value for field stars (cross) with laboratory data from Sandford *et al.* (squares). Water-ice mixtures (within box at top right) are: (1) $H_2O:CO = 20:1$, (2) $H_2O:CO = 140:1$, (3) $H_2O:CO:CH_4 = 20:1:2$, (4) $H_2O:CO:CH_3OH = 20:1:2$, (5) $H_2O:CO:NH_3 = 100:2:1$ and (6) $H_2O:CH_3OH:CO:NH_3 = 100:50:1:1$. The $CO_2:CO$ ratio is 20:1.

value of 4.673 μm is significant, and effectively rules out a water-ice matrix as host for the CO molecules responsible for the narrow component of the observed feature, dominant in our spectra. Water-based mantle material is likely to account for the weaker broad component of the feature (Sandford *et al.* 1988). Of the mixtures studied by Sandford *et al.*, that which lies closest to the observations in Fig. 6 is $CO_2:CO$ ($\lambda_0 \simeq 4.674$ μm, $\Delta\nu_{1/2} \simeq 5.8$ cm^{-1}).

Models for the accretion of grain mantles suggest that two types of mantle composition should be produced, dependent on the ratio of atomic to molecular hydrogen (Allamandola & Sandford 1988). In environments rich in H I, the mantle is dominated by polar molecules such as H_2O and NH_3, whereas in molecular clouds, the mantle material is composed predominantly of non-polar species such as O_2 and N_2. Allamandola & Sandford argue that the broad and narrow components of the CO feature are produced in the polar and non-polar ices, respectively. Whereas water-dominated mantles provide a natural explanation for the broad copmponent, the origin of the narrow component is more problematic. CO_2 is produced easily in the laboratory by ultraviolet photolysis of pure solid CO (e.g. d'Hendecourt *et al.* 1986), but this process presumably cannot operate efficiently deep within a dark cloud. Other non-polar molecules, such as N_2 and CH_4, may be abundant in the mantles. Interestingly, the laboratory spectrum reported by Maki (1961) for $CH_4:CO$ at 30 K has $\lambda_0^{-1} \sim 2139.3$ cm^{-1} and $\Delta\nu_{1/2} \sim 8$ cm^{-1}, in excellent agreement with the observations; however, the $CH_4:CO$ spectrum obtained by Sandford *et al.* disagrees significantly in both position and width with that of Maki.

4 Column densities and depletions

4.1 SOLID CO COLUMN DENSITIES

The column density $N_{dust}(CO)$ condensed on to dust grains is deduced in a straightforward way from the optical depth, width and intrinsic strength of the 4.67-μm feature (Lacy *et al.* 1984; Sandford *et al.* 1988), using the formula

$$N_{dust}(CO) = \frac{\tau_{4.67}\Delta\nu_{1/2}}{A}, \tag{4}$$

where A is the absorption intensity in cm molecule^{-1}. A is sensitive to both the composition and the thermal history of the ice matrix containing the CO (see also Schmitt *et al.* 1989). Sandford *et al.* report values of $A \sim 1.0 \times 10^{-17}$ for the 2139 cm^{-1} line of pure CO and $A \sim 1.7 \times 10^{-17}$ for the 2136 cm^{-1} H_2O:CO feature (unannealed at 10 K). Unfortunately, no A-value is available for the CO_2:CO mix discussed in the previous section, and we adopt the result for pure CO in our analysis. Possible systematic errors of factor ~ 2 may thus be associated with the uncertainty in A.

We deduce $N_{dust}(CO)$ from equation (4) using the values of $\tau_{4.67}$ and $\Delta\nu_{1/2}$ listed in Table 2; results are presented in the final column of Table 2.

4.2 COMPARISON WITH GAS PHASE DATA

Ideally, the degree of depletion of CO on to grains is measured by means of a direct comparison of column densities $N_{gas}(CO)$ and $N_{dust}(CO)$ in the same line-of-sight, deduced by absorption spectroscopy of a background source. In principle, $N_{gas}(CO)$ may be evaluated towards those stars for which we have $N_{dust}(CO)$ data by observing the gas-phase interstellar absorption lines in the fundamental vibration–rotation bands. However, this is difficult in practice because very high spectral resolution ($\lambda/\Delta\lambda > 10^4$) is required to separate telluric and interstellar features, and studies are limited to bright sources with existing technology (e.g. Mitchell, Allen & Maillard 1988). An alternative is to use millimetre-wave observations of CO *emission* to estimate $N_{gas}(CO)$. However, there are two potential problems associated with this approach. First, the millimetre lines of the more abundant CO isotopes are generally saturated, and isotope ratios must be assumed to obtain results based on the less abundant isotopes. Secondly, the volume of space sampled may be different: for example, differences in beam size can introduce errors if the density changes across the line-of-sight, and, more seriously, material behind the infrared source may contribute to the molecular emission and thus reduce the apparent depletion. No infrared obesrvations of gas-phase CO are available to date for the stars discussed in this paper, but extensive millimetre-wave data have been published by Frerking, Langer & Wilson (1982) for the lines-of-sight to all of the field stars catalogued by Elias (1978). As the Taurus cloud is $\sim 20°$ out of the galactic plane, background molecular emission in the beam is unlikely to be a significant problem for lines-of-sight to stars which are themselves background to the dark cloud.

Table 3 presents estimates of gas-phase column densities based on millimetre-wave data from Frerking *et al.* (1982) for Elias stars, and from Crutcher (1985) for HD 29647. Measurements of $N(^{12}C^{18}O)$, $N(^{12}C^{17}O)$ and $N(^{13}C^{18}O)$ are converted to $N(^{12}C^{16}O)$ using standard terrestrial isotope ratios. The adopted value (weighted to the result for the least abundant isotope observed in each case) is given in the final column. Fig. 7 shows a plot of $N_{dust}(CO)$ (Table 2) against $N_{gas}(CO)$ (Table 3). Significant linear correlation is apparent, and for more highly obscured sources, $N_{dust}(CO)/N_{gas}(CO) \sim 0.3$.

Table 3. Gas-phase column densities towards field stars.

Star	N_{gas}(CO)*			N_{gas}(CO)
	[1]	[2]	[3]	Adopted
Elias 3	2.9–6.5	4.1–6.5	—	5.3 ± 1.2
Elias 6	2.4–4.9	4.6–8.1	—	6.4 ± 1.8
Elias 13	3.6–15.8	6.5–13.5	—	10.0 ± 3.5
Elias 14	1.8–3.5	3.5–6.2	—	4.9 ± 1.4
Elias 15	> 5.3	8.4–19.4	8.4–15.0	11.7 ± 3.3
Elias 16	> 5.4	8.4–18.4	12.8–23.8	18.3 ± 5.0
HD29647	4.8 ± 1.0	—	—	4.8 ± 1.0

*Key to column densities:

[1] = 4.9×10^2 $N(^{12}C^{18}O)$,
[2] = 2.7×10^3 $N(^{12}C^{17}O)$,
[3] = 4.4×10^4 $N(^{13}C^{18}O)$,
(Units: 10^{17} cm^{-2}).

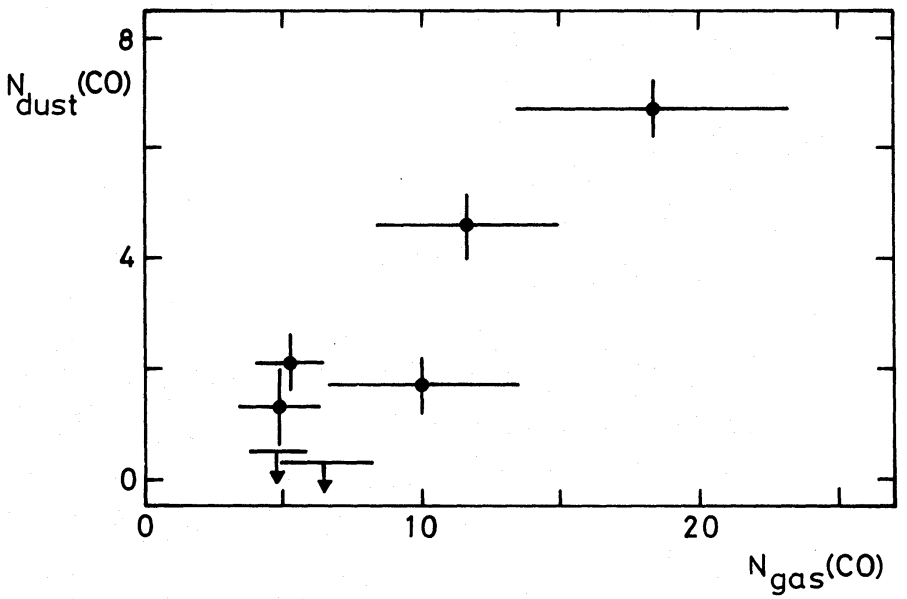

Figure 7. Plot of CO column density for dust, deduced from the 4.67-μm feature, against that for the gas, based on millimetre-wave data for the same lines-of-sight. Units are 10^{17} cm^{-2}.

4.3 DISCUSSION

In lines-of-sight towards luminous, embedded 'protostellar' objects, the average depletion of CO appears to be low, with $N_{dust}(CO)/N_{gas}(CO) \leq 0.05$. This result is well-established in the lines-of-sight to NGC 2024 no. 2 and W33A (Geballe 1986 and Mitchell *et al.* 1988, respectively) on the basis of direct comparison of infrared absorption spectra for both dust and gas. In a number of similar objects (BN, OMC-1 IRc2, GL2591), the solid CO feature is undetected at a level below that expected if a substantial fraction of the observed gas-phase CO were depleted. These regions are very probably heated by the embedded sources within them, and are unlikely to be representative of the quiescent dark-cloud environment.

In quiescent clouds, models suggest that CO should become almost totally depleted on time-scales less than cloud lifetimes in the absence of any efficient desorption mechanism (e.g. Léger 1983). Our investigation suggests that in Taurus, the depletion is modest (~ 30 per cent), and independent of optical depth for $A_V > 5$ mag. The implications of this result are discussed in

detail elsewhere (Duley *et al.* 1989). If we assume that the refractory component of the grain material is amorphous, localized heating of subunits or islands within the grain structure due to the absorption of individual photons can act as an efficient desorption mechanism. The existence of threshold extinctions for detection of H_2O and CO ices are then easily understood if the cloud is heated predominantly by the external interstellar radiation field. Deep within the cloud, cosmic rays are likely to be the most significant source of energy contributing to desorption from grain surfaces, and Duley *et al.* argue that the ultraviolet field produced by cosmic ray excitation of H_2 can account for the observed abundances of CO on grains and in the gas phase.

5 Conclusions

The principal results of this paper are as follows.

(i) The optical depth of the solid CO feature correlates closely with visual extinction, and with the depth of the 3-μm ice band. Threshold effects indicate the existence of three distinct regimes in the Taurus cloud: an outer skin ($0 < A_V < 3.3$) in which no volatile mantles occur, an intermediate layer ($3.3 < A_V < 5.3$), in which H_2O condenses but CO remains predominantly in the gas, and an inner region ($A_V > 5.3$) in which both water-ice and solid CO are present in grain mantles.

(ii) The position and width of the observed CO feature exclude an origin in mantles with H_2O as the main constituent. This strongly suggests that grain growth is hierarchical, with an inner H_2O-dominated mantle enclosed within an outer mantle containing CO in a matrix dominated by non-polar molecules. A small concentration of CO in the H_2O-rich mantles may account for the broad component of the feature, centred at $\sim 2136\ \mathrm{cm}^{-1}$.

(iii) From a comparison of infrared and millimetre-wave data for solid- and gas-phase CO, the degree of depletion appears to be ~30 per cent for stars with visual extinctions in the range $5 < A_V < 21$.

In order to capitalize on the potential of the 4.67-μm feature as a diagnostic of the physics and chemistry of grain mantles, it will be necessary, in the future, to obtain observational profiles at higher spectral resolution and signal-to-noise than those presented here. Detailed modelling of the profiles will require new laboratory data for CO embedded in ices composed of abundant non-polar molecules, and measurements of the absorption intensity of the feature in such mixes are needed to refine column density estimates. Finally, high-resolution spectroscopy of gas-phase interstellar CO absorption lines should be attempted for the Taurus stars, in order to check the reliability of the depletions based on millimetre-wave emission.

Acknowledgments

This research is supported by grants from the North Atlantic Treaty Organization, the Natural Sciences and Engineering Research Council of Canada and the Science and Engineering Research Council (UK). AJA holds an assistantship funded by the National Advisory Body for research in polytechnics. The United Kingdom Infrared Telescope is operated by the Royal Observatory, Edinburgh, on behalf of the SERC.

References

Adamson, A. J., Whittet, D. C. B., Bode, M. F., Longmore, A. J., Roche, P. F., McFadzean, A. D., Geballe, T. R. & Aitken, D. K., 1988. In: *Dust in the Universe,* p. 61, eds Bailey, M. E. & Williams, D. A., Cambridge University Press.

Allamandola, L. J. & Sandford, S. A., 1988. In: *Dust in the Universe,* eds Bailey, M. E. & Williams, D. A., Cambridge University Press, Cambridge.
Crutcher, R. M., 1985. *Astrophys. J.,* **288,** 604.
d'Hendecourt, L. B., Allamandola, L. J., Grim, R. J. A. & Greenberg, J. M., 1986. *Astr. Astrophys.,* **158,** 119.
Duley, W. W., 1974. *Astrophys. Space Sci.,* **26,** 199.
Duley, W. W., Jones, A. P., Whittet, D. C. B. & Williams, D. A., 1989. *Mon. Not. R. astr. Soc.,* in press.
Eiroa, C. & Hodapp, K. W., 1989. *Astr. Astrophys.,* **210,** 345.
Elias, J. H., 1978. *Astrophys. J.,* **224,** 857.
Frerking, M. A., Langer, W. D. & Wilson, R. W., 1982. *Astrophys. J.,* **262,** 590.
Geballe, T. R., 1986. *Astr. Astrophys.,* **162,** 248.
Lacy, J. H., Baas, F., Allamandola, L. J., Persson, S. E., McGregor, P. J., Lonsdale, C. J., Geballe, T. R. & van de Bult, C. E. P., 1984. *Astrophys. J.,* **276,** 533.
Léger, A., 1983. *Astr. Astrophys.,* **123,** 271.
Maki, A. G., 1961. *J. Chem. Phys.,* **35,** 931.
Mitchell, G. F., Allen, M. & Maillard, J. P., 1988. *Astrophys. J.,* **333,** L55.
Sandford, S. A., Allamandola, L. J., Tielens, A. G. G. M. & Valero, G. J., 1988. *Astrophys. J.,* **329,** 498.
Schmitt, B., Greenberg, J. M. & Grim, R. J. A., 1989. *Astrophys. J.,* **340,** L33.
van Dischoeck, E. F. and Black, J. H., 1987. In: *Physical Processes in Interstellar Clouds,* p. 241, eds Morfill, G. E. & Scholer, M., Reidel, Dordrecht.
Whittet, D. C. B., 1987. *Q. Jl R. astr. Soc.,* **28,** 303.
Whittet, D. C. B., Bode, M. F., Longmore, A. J., Baines, D. W. T. & Evans, A., 1983. *Nature,* **303,** 218.
Whittet, D. C. B., Longmore, A. J. & McFadzean, A. D., 1985. *Mon. Not. R. astr. Soc.,* **216,** 45P (Paper I).
Whittet, D. C. B., Bode, M. F., Longmore, A. J., Adamson, A. J., McFadzean, A. D., Aitken, D. K. & Roche, P. F., 1988. *Mon. Not. R. astr. Soc.,* **233,** 321 (Paper II).